INTERNATIONAL JOURNAL FOR NUMERICAL METHODS IN FLUIDS, VOL. 5, 81–97 (1985)

COMPUTATION OF HIGH SPEED TURBULENT BOUNDARY-LAYER FLOWS USING THE k–ε TURBULENCE MODEL

A. LIAKOPOULOS

Department of Engineering Sciences, University of Florida, Gainesville, Florida 32611, U.S.A.

SUMMARY

The applicability of a finite element–differential method to the computation of steady two-dimensional low-speed, transonic and supersonic turbulent boundary-layer flows is investigated. The turbulence model chosen for the Reynolds shear stress and turbulent heat flux is the k–ε two-equation model. Calculations are extended up to the wall and the exact values of the dependent variables at the wall are used as boundary conditions. A number of transformations are carried out and the assumed solutions at a longitudinal station are represented by complete cubic spline functions. In essence, the method converts the governing partial differential equations into a system of ordinary differential equations by a weighted residuals method and invokes an ordinary differential equation solver for the numerical integration of the reduced initial-value problem. The results of the computations reveal that the method is highly accurate and efficient. Furthermore, the accuracy and applicability of the k-ε turbulence model are examined by comparing results of the computations with experimental data. The agreement is very good.

KEY WORDS Compressible Flow Turbulent Flow Boundary Layers Galerkin Method Spline Functions

INTRODUCTION

The development of a general calculation procedure for turbulent boundary-layer flows has been the objective of numerous research efforts. Since the computation of an entire flow field by direct numerical solution of the time dependent conservation equations is at present impossible, the usual point of departure in practical applications is an averaged version of the conservation equations. The averaged equations involve new unknown variables which must be modelled. The computations presented in this study were carried out using the k–ε two-equation turbulence model which has become very popular in computing incompressible turbulent flows. However, its application to compressible flows has received little attention.[1,2] The present paper is mainly concerned with boundary-layer flows which are influenced in an important way by compressibility. In contrast with previous work calculations are extended up to the wall and the exact values of the dependent variables at the wall are used as boundary conditions.

The coupling of the k-ε turbulence model with the averaged conservation equations leads to a parabolic system of partial differential equations. Consequently, numerical methods initially developed for incompressible laminar boundary-layer flow problems can be used for the solution of turbulent flow problems on the condition that they provide means for coping with at least two major characteristics of turbulent boundary layers that require special numerical treatment: the high rate of the boundary-layer thickness growth and the very large gradients occurring at the immediate vicinity of the wall. In addition, profiles for turbulence quantities at the initial station for

0271–2091/85/01 0081–17$01.70

Received 27 January 1984
Revised 26 March 1984

arbitrary Reynolds number, Mach number and wall temperature conditions are required. Provision of these profiles can be difficult owing to the lack of experimental data or *a priori* knowledge of the behaviour of the model predictions.

A large variety of numerical methods for solving parabolic partial differential equations have been used to calculate boundary-layer flows with various levels of success. The Hartree–Womersley method[3] has been employed by Smith and Clutter[4] to solve the equations for laminar boundary layers and by Herring and Mellor[5] for turbulent flows. Finite-difference schemes, ranging from simple conventional ones to more sophisticated variants, have been used extensively. Pletcher[6,7] used the DuFort–Frankel explicit scheme to calculate incompressible and compressible turbulent boundary layers. Implicit schemes of Crank–Nicolson type have been applied to compressible turbulent boundary layers by Harris[8] and Cebeci *et al.*[9] among others. Patankar and Spalding[10] obtained a finite-difference scheme by expressing each term in the governing equations as an integrated average over a small control volume defined by the grid. Keller and Cebeci[11] successfully applied the box-scheme to boundary-layer flow problems. In general, finite-difference schemes although simple, easily formulated and accurate, require special measures in selecting the grid size in the vicinity of a separation point, because the separation point of a boundary-layer flow is not known beforehand. Applications of the finite element method to turbulent boundary layers have been reported among others by Soliman and Baker[12] and Fletcher and Fleet.[13]

In the present work, the accuracy and efficiency of a finite element–differential method proposed by Hsu[14] and extensively tested in laminar flows[15] is investigated for the class of compressible turbulent boundary-layer flows. A number of appropriate transformations are first carried out. The transformed flow region is divided into a number of strips parallel to the body surface and the unknown functions at a longitudinal station are represented by complete cubic splines. The governing partial differential equations are then reduced to a system of first-order non-linear ordinary differential equations by a weighted residual method and the reduced initial-value problem is numerically integrated by an ordinary differential equation solver.

The method is applied to low-speed, transonic and supersonic flows. The obtained results show that the finite element–differential method is very efficient and accurate provided that a very limited number of numerical parameters are properly selected.

The paper is built up as follows. In Section 2 the governing equations for the flows considered are presented, and in Section 3 attention is focused upon the turbulence model and its applicability to compressible flows. In Section 4 alternative forms of the boundary-layer governing equations are introduced, and in Section 5 the method of solution is described. Numerical results for several boundary-layer flows are presented in Section 6.

2. GOVERNING EQUATIONS

For the class of steady, two-dimensional, compressible, turbulent, perfect gas boundary-layer flows the governing equations, neglecting body forces, are[16]

$$\frac{\partial}{\partial x}(\bar{\rho}\bar{u}) + \frac{\partial}{\partial y}(\overline{\rho v}) = 0 \tag{1}$$

$$\bar{\rho}\bar{u}\frac{\partial \bar{u}}{\partial x} + \overline{\rho v}\frac{\partial \bar{u}}{\partial y} = -\frac{\mathrm{d}p_e}{\mathrm{d}x} + \frac{\partial}{\partial y}\left(\bar{\mu}\frac{\partial \bar{u}}{\partial y} - \bar{\rho}\overline{u'v'}\right) \tag{2}$$

$$\bar{\rho}\bar{u}\frac{\partial \bar{H}}{\partial x} + \overline{\rho v}\frac{\partial \bar{H}}{\partial y} = \frac{\partial}{\partial y}\left[\frac{Pr-1}{Pr}\bar{\mu}\frac{\partial}{\partial y}\left(\frac{\bar{u}^2}{2}\right) + \frac{\bar{\mu}}{Pr}\frac{\partial \bar{H}}{\partial y} - \bar{\rho}\overline{v'H'}\right] \tag{3}$$

$$\bar{p} = \bar{\rho}R\bar{T} = \bar{\rho}R\left(\bar{H} - \frac{\bar{u}^2}{2}\right)\Big/ c_p \tag{4}$$

where

x = co-ordinate along the body surface
y = co-ordinate normal to the body surface
u = velocity component in x-direction
v = velocity component in y-direction
ρ = local fluid density
H = total enthalpy
μ = dynamic viscosity
Pr = molecular Prandtl number of the fluid
p = static pressure
R = gas constant
c_p = specific heat at constant pressure

In equations (1)–(4) bars denote conventional time-averages, primes denote fluctuations and the subscript e refers to conditions in the external flow field.

3. THE TURBULENCE MODEL

In order to solve the system of equations (1)–(4) closure assumptions must be made for the Reynolds shear stress, $-\bar{\rho}\overline{u'v'}$, and the turbulent heat flux $-\bar{\rho}\overline{v'H'}$. In the k–ε two-equation turbulence model, developed for incompressible flows by Jones and Launder,[17,18] the Reynolds shear stress and turbulent heat flux are related to the mean velocity and total enthalpy fields by

$$-\rho\overline{u'v'} = \mu_T \frac{\partial \bar{u}}{\partial y} \tag{5}$$

$$-\rho\overline{v'H'} = \frac{\mu_T}{Pr_T}\frac{\partial \bar{H}}{\partial y} \tag{6}$$

where μ_T is the turbulent (eddy) viscosity and Pr_T is the turbulent Prandtl number. The turbulent viscosity μ_T is expressed in terms of the turbulence kinetic energy, k, and dissipation rate, ε, by

$$\mu_T = C_\mu f_\mu \rho \frac{k^2}{\varepsilon} \tag{7}$$

and the system is 'closed' by introducing transport equations for the turbulence kinetic energy and dissipation rate:

$$\rho\frac{Dk}{Dt} = \frac{\partial}{\partial y}\left(\mu_k \frac{\partial k}{\partial y}\right) + \mu_T\left(\frac{\partial \bar{u}}{\partial y}\right)^2 - \rho\varepsilon - 2\bar{\mu}\left(\frac{\partial k^{1/2}}{\partial y}\right)^2 \tag{8}$$

$$\rho\frac{D\varepsilon}{Dt} = \frac{\partial}{\partial y}\left(\mu_\varepsilon \frac{\partial \varepsilon}{\partial y}\right) + c_1 f_1 \mu_T \frac{\varepsilon}{k}\left(\frac{\partial \bar{u}}{\partial y}\right)^2 - c_2 f_2 \rho \frac{\varepsilon^2}{k} + 2\bar{\nu}\mu_T\left(\frac{\partial^2 \bar{u}}{\partial y^2}\right)^2 \tag{9}$$

In equations (7)–(9) modifications for the low turbulence Reynolds number region very close to the wall have been incorporated so that calculations can be extended up to the wall. The values of the empirical 'constants' C_μ, c_1, c_2, σ_k, σ_ε and the functions f_μ, f_1, f_2 are taken to be[17]

$$C_\mu = 0{\cdot}09, c_1 = 1{\cdot}55, c_2 = 2{\cdot}0, \sigma_k = 1{\cdot}0, \sigma_\varepsilon = 1{\cdot}3 \tag{10}$$
$$f_1 = 1{\cdot}0, f_2 = 1 - 0{\cdot}3\exp(-R_T^2), f_\mu = \exp[-2{\cdot}5/(1 + 0{\cdot}02R_T)]$$

In the above, $R_T = \rho k^2/\mu\varepsilon$, $\mu_k = \bar{\mu} + \mu_T/\sigma_k$, $\mu_\varepsilon = \bar{\mu} + \mu_T/\sigma_\varepsilon$ and ν denotes the kinematic viscosity.

It is assumed that the forms of the turbulence transport equations and the modelling constants

remain unchanged when the model is applied to compressible flows. Compressibility effects are accounted for by interpreting the dependent variables as mass-weighted averaged variables and by using the local mean density in both conservation and turbulence transport equations. It should be noted that formal application of mass-weighted averaging to the exact transport equations of turbulence kinetic energy and dissipation rate leads to partial differential equations that contain more terms than their incompressible counterparts. Experience with modelling the additional terms indicates that their influence on the quality of predictions is small.[19,20] The viewpoint adopted here is that the additional terms in the k and ε equations can be neglected without significant loss of accuracy. The resulting model is shown to be sufficiently complete to give good agreement with experimental data, yet simple enough to be computationally tractable.

In the sequel, some implications of the modelling assumptions related to compressibility are presented by analysing the logarithmic-law region of a compressible boundary-layer flow past a smooth insulated flat plate at zero incidence. In this region, convection as well as molecular diffusion are negligible and the production of turbulence kinetic energy is equal to dissipation. Under these conditions, equations (2), (8) and (9) become

$$C_\mu \bar{\rho} \frac{k^2}{\varepsilon} \frac{\partial \bar{u}}{\partial y} = \rho_w u_\tau^2 \tag{11}$$

$$C_\mu k^2 \left(\frac{\partial \bar{u}}{\partial y} \right)^2 = \varepsilon^2 \tag{12}$$

and

$$\frac{\partial}{\partial y}\left[\frac{C_\mu}{\sigma_\varepsilon} \bar{\rho} \frac{k^2}{\varepsilon} \frac{\partial \varepsilon}{\partial y} \right] + c_1 C_\mu \bar{\rho} k \left(\frac{\partial \bar{u}}{\partial y} \right)^2 - c_2 \bar{\rho} \frac{\varepsilon^2}{k} = 0 \tag{13}$$

where u_τ denotes the friction velocity and subscript w denotes conditions at the wall. Furthermore, the non-dimensional generalized velocity

$$u^+ = \frac{u^*}{u_\tau} = \frac{1}{u_\tau} \int_0^u \left(\frac{\rho}{\rho_w} \right)^{1/2} \mathrm{d}u$$

obeys the usual incompressible logarithmic law

$$u^+ = \frac{1}{\kappa} \ln y^+ + B \tag{14}$$

where κ and B are constants.

Let

$$k^* = \left(\frac{\rho}{\rho_w} \right)^m k \quad \text{and} \quad \varepsilon^* = \left(\frac{\rho}{\rho_w} \right)^n \varepsilon \tag{15}$$

Substitution of (14) and (15) into equations (11) and (12) yields the relations

$$C_\mu \left(\frac{\rho_w}{\rho} \right)^{2m-n-1/2} \frac{k^{*2}}{\varepsilon^*} \frac{\mathrm{d}u^*}{\mathrm{d}y} = u_\tau^2 \quad \text{and} \quad C_\mu \left(\frac{\mathrm{d}u^*}{\mathrm{d}y} \right) = \left(\frac{\rho_w}{\rho} \right)^{-2m+2n-1} \frac{k^{*2}}{\varepsilon^{*2}} \tag{16}$$

which reduce to the corresponding incompressible forms for $m = 1$ and $n = 3/2$. Consequently, the distributions of the dimensionless k^* and ε^* in the logarithmic-law region are given by the formulae of incompressible flow, i.e.

$$k^+ = C_\mu^{-1/2} \quad \text{and} \quad \varepsilon^+ = \frac{1}{\kappa y^+} \tag{17}$$

where $k^+ = k^*/u_\tau^2$ and $\varepsilon^+ = \varepsilon^* \nu_w / u_\tau^4$.

By substituting equations (14) and (17) in equation (13) and using the relation $\rho_w T_w = \rho T$ one obtains

$$\frac{k^2}{\sigma_\varepsilon} + (c_1 - c_2)\sqrt{C_\mu} + \frac{k^2}{\sigma_\varepsilon}\left(\frac{3}{2}\frac{y^2}{T}\frac{\partial^2 T}{\partial y^2} - \frac{y}{T}\frac{\partial T}{\partial y}\right) = 0 \tag{18}$$

For a boundary-layer flow over an adiabatic wall, the generalized velocity is given by

$$u^* = \frac{u_e}{m}\sin^{-1}\left(m\frac{\bar{u}}{u_e}\right) \tag{19}$$

where

$$m^2 = \frac{\frac{1}{2}(\gamma - 1)M_e^2}{1 + \frac{1}{2}(\gamma - 1)M_e^2}$$

and the temperature distribution, assuming $Pr = 1$ for simplicity, by

$$\frac{T}{T_e} = 1 + \tfrac{1}{2}(\gamma - 1)M_e^2\left[1 - \left(\frac{\bar{u}}{u_e}\right)^2\right] \tag{20}$$

where γ is the specific heat ratio and M denotes the Mach number. After combining equation (18) with equations (19) and (20) and a good deal of algebra, equation (13) becomes

$$\frac{k^2}{\sigma_\varepsilon} + (c_1 - c_2)\sqrt{c_\mu} + \frac{u_\tau}{u_e}\left[A_1\frac{\kappa}{m}\sin\left(2m\frac{u^*}{u_e}\right)\right] - \left(\frac{u_\tau}{u_e}\right)^2 A_1\cos\left(2m\frac{u^*}{u_e}\right) = 0$$

where

$$A_1 = \frac{-(\gamma - 1)T_e M_e^2}{4T\sigma_\varepsilon}$$

As $Re \to \infty$, $u_\tau/u_e \to 0$ and consequently equation (13) is satisfied by the modelling constants for incompressible flows. Furthermore, it is evident from equations (17) that in the logarithmic-law region of a compressible boundary layer the turbulence length scale, $l = C_\mu k^{3/2}/\varepsilon$, reduces to its incompressible form, $l = C_\mu^{1/4}\kappa y$, i.e. the turbulence structure is unaffected by compressibility. According to Morkovin's hypothesis[21] this is valid in boundary-layer flows of Mach number less than 5. Consequently, one expects that our modelling assumptions concerning compressibility effects on turbulence hold in the non-hypersonic flow regime. However, the validity of the adopted approach can be assessed only by comparing computations and measurements of experimentally documented flows.

4. THE TRANSFORMED INITIAL BOUNDARY VALUE PROBLEM

Equations (1)–(9) constitute the set of governing equations for the class of flows considered in this work. The associated boundary and initial conditions considered are

$$y = 0: \bar{u} = \overline{\rho v} = k = \varepsilon = 0,\ \bar{H} = \bar{H}_w(x) \tag{21}$$

$$y \to \infty: \bar{u} \to u_e(x),\ \bar{H} \to H_e(x),\ k \to k_e(x),\ \varepsilon \to \varepsilon_e(x) \tag{22}$$

$$x = x_0: \bar{u} = \bar{u}_i(y),\ \bar{H} = \bar{H}_i(y),\ k = k_i(y),\ \varepsilon = \varepsilon_i(y) \tag{23}$$

where k_e and ε_e are given by the solution of the following system of differential equations

$$u_e\frac{dk_e}{dx} = -\varepsilon_e, \quad u_e\frac{d\varepsilon_e}{dx} = -c_2\frac{\varepsilon_e^2}{k_e} \tag{24}$$

Although it is possible to devise numerical techniques to solve the boundary-layer equations in physical co-ordinates,[22] it is advantageous especially from the computational point of view to carry out a number of co-ordinate transformations and obtain alternative forms of the boundary-layer equations. Using appropriate co-ordinate transformations one can overcome, to some extent, numerical difficulties caused by the boundary-layer thickness increase in the streamwise direction and the presence of a singularity at the tip of a sharp body. After carrying out a number of co-ordinate transformations described in detail in Reference 23* the governing equations become

$$\frac{\partial w}{\partial \xi} = \frac{\eta}{4}\frac{\partial w}{\partial \eta} + \frac{w^{1/2}}{4\eta^2}\left[\alpha_1\left(\frac{\partial^2 w}{\partial \eta^2} - \frac{1}{\eta}\frac{\partial w}{\partial \eta}\right) + \alpha_2\frac{\partial w}{\partial \eta}\right] + 2[(1-w) + \theta(\xi)(1-\phi^{1/2})]\frac{\mathrm{d}\ln U(\xi)}{\mathrm{d}\xi} \tag{25}$$

$$\frac{\partial \phi}{\partial \xi} = \frac{\eta}{4}\frac{\partial \phi}{\partial \eta} + \frac{w^{1/2}}{4\eta^2}\left[\alpha_3\left(\frac{\partial^2 \phi}{\partial \eta^2} - \frac{1}{\eta}\frac{\partial \phi}{\partial \eta} + \frac{1}{2}\frac{\partial \phi}{\partial \eta}\frac{\partial \ln\left(\frac{w}{\phi}\right)}{\partial \eta}\right) + \alpha_4\frac{\partial \phi}{\partial \eta}\right] \tag{26}$$

$$- q(\xi)\frac{(\phi w)^{1/2}}{4\eta^2}\left[\alpha_5\left(\frac{\partial^2 w}{\partial \eta^2} - \frac{1}{\eta}\frac{\partial w}{\partial \eta} + \frac{1}{2w}\left(\frac{\partial w}{\partial \eta}\right)^2\right) + \alpha_6\frac{\partial w}{\partial \eta}\right] + 2(\phi^{1/2} - \phi)\frac{\mathrm{d}\ln\theta(\xi)}{\mathrm{d}\xi}$$

$$\frac{\partial k}{\partial \xi} = \frac{\eta}{4}\frac{\partial k}{\partial \eta} + \frac{w^{1/2}}{4\eta^2}\left[\alpha_7\left(\frac{\partial^2 k}{\partial \eta^2} - \frac{1}{\eta}\frac{\partial k}{\partial \eta} + \frac{1}{2w}\frac{\partial w}{\partial \eta}\frac{\partial k}{\partial \eta}\right) + \alpha_8\frac{\partial k}{\partial \eta}\right] \tag{27}$$

$$- \tfrac{1}{8}\lambda_4\mu_4\frac{w^{1/2}}{k\eta^2}\left(\frac{\partial k}{\partial \eta}\right)^2 + \frac{A(\xi)\lambda_4\mu_{T4}}{\eta^2 w^{1/2}}\left(\frac{\partial w}{\partial \eta}\right)^2 - \frac{B(\xi)\varepsilon}{w^{1/2}}$$

$$\frac{\partial \varepsilon}{\partial \xi} = \frac{\eta}{4}\frac{\partial \varepsilon}{\partial \eta} + \frac{w^{1/2}}{4\eta^2}\left[\alpha_9\left(\frac{\partial^2 \varepsilon}{\partial \eta^2} - \frac{1}{\eta}\frac{\partial \varepsilon}{\partial \eta} + \frac{1}{2w}\frac{\partial w}{\partial \eta}\frac{\partial \varepsilon}{\partial \eta}\right) + \alpha_{10}\frac{\partial \varepsilon}{\partial \eta}\right] \tag{28}$$

$$- \frac{C(\xi)f_2\varepsilon^2}{kw^{1/2}} + \frac{D(\xi)\varepsilon}{k\eta^2 w^{1/2}}\lambda_4\mu_{T4}\left(\frac{\partial w}{\partial \eta}\right)^2 + E(\xi)\mu_4\mu_{T4}\frac{w^{1/2}}{\eta^4}\left[\frac{\partial w}{\partial \eta}\frac{\partial \lambda_4}{\partial \eta} + \lambda_4\left(\frac{\partial^2 w}{\partial \eta^2} - \frac{1}{\eta}\frac{\partial w}{\partial \eta}\right)\right]^2$$

in which

$$\lambda_4 = \frac{T_0}{T(\xi,\eta)}$$

$$\alpha_1 = \lambda_4(\mu_4 + \mu_{T4}) = \lambda_4\mu_{u4}, \qquad \alpha_2 = \frac{\partial \alpha_1}{\partial \eta}$$

$$\alpha_3 = \lambda_4\left(\frac{\mu_4}{Pr} + \frac{\mu_{T4}}{Pr_T}\right) = \lambda_4\mu_{H4}, \qquad \alpha_4 = \frac{\partial \alpha_3}{\partial \eta}$$

$$\alpha_5 = \frac{Pr - 1}{Pr}\lambda_4\mu_4, \qquad \alpha_6 = \frac{\partial \alpha_5}{\partial \eta}$$

$$\alpha_7 = \lambda_4\left(\mu_4 + \frac{\mu_{T4}}{\sigma_k}\right) = \lambda_4\mu_{k4} \qquad \alpha_8 = \frac{\partial \alpha_7}{\partial \eta}$$

$$\alpha_9 = \lambda_4\left(\mu_4 + \frac{\mu_{T4}}{\sigma_\varepsilon}\right) = \lambda_4\mu_{\varepsilon 4}, \qquad \alpha_{10} = \frac{\partial \alpha_9}{\partial \eta}$$

*Besides the well known Illingworth–Stewartson, von Mises, and Falkner–Skan, additional co-ordinate transformations are employed to improve the efficiency of the computational procedure.

$$s(\xi)=\frac{T_e(\xi)}{T_0}=\frac{2H_0}{2H_0+U_\infty^2U^2(\xi)}$$

$$\beta(\xi)=\frac{p_e}{p_0}\left(\frac{c_e}{c_0}\right)^2=[s(\xi)]^{(2\gamma-1)/(\gamma-1)}$$

$$q(\xi)=\frac{2U_\infty^2U^2(\xi)}{2H_0+U_\infty^2U^2(\xi)}\frac{1}{\theta(\xi)},\qquad A(\xi)=\frac{U_\infty^2}{16k_r}s(\xi)U^2(\xi)$$

$$B(\xi)=\frac{\varepsilon_rL(\upsilon e^{\xi})}{U_\infty k_r\beta(\xi)U^2(\xi)},\qquad C(\xi)=c_2B(\xi)$$

$$D(\xi)=c_1f_1A(\xi),\qquad E(\xi)=\frac{U_\infty^3\beta(\xi)U^4(\xi)s(\xi)}{32\varepsilon_rL(\upsilon e^{\xi})}$$

In the above $w(\xi,\eta)$ and $\phi(\xi,\eta)$ are the transformed velocity and enthalpy, respectively, and $U(\xi)$ and $\theta(\xi)$ are related to the boundary conditions and reference parameters. Furthermore, c denotes the speed of sound, and υ, L, k_r, ε_r are transformation constants. The subscript 0 refers to stagnation conditions in the external stream, subscript ∞ to conditions at infinity, and subscript 4 signifies the number of transformation sets used in the present work. It should be pointed out that the number of differential equations has been reduced by one through the use of von Mises transformation.

The boundary and initial conditions, equations (21)–(23), become

$$\eta=0: w=\phi=k=\varepsilon=0 \tag{29}$$

$$\eta\to\infty: w\to 1,\ \phi\to 1,\ k\to k_e(\xi),\ \varepsilon\to\varepsilon_e(\xi) \tag{30}$$

$$\xi=\xi_0: w=w_i(\eta),\ \phi=\phi_i(\eta),\ k=k_i(\eta),\ \varepsilon=\varepsilon_i(\eta) \tag{31}$$

The local skin-friction coefficient and the heat-transfer coefficient defined as

$$c_f(x)=\frac{\tau_w(x)}{\frac{1}{2}\rho_eu_e^2}\quad\text{and}\quad c_q(x)=\frac{q_w(x)}{\rho_eu_ec_pT_{0e}}$$

become

$$c_f(\xi)=\frac{\mu_w}{\mu_0}\frac{\rho_w}{\rho_e}\frac{w_0''}{2(Re\,\upsilon e^{\xi})^{1/2}}$$

$$c_q(\xi)=\frac{1}{Pr}\frac{\mu_w\rho_w}{\mu_0\rho_e}\frac{\theta(\xi)}{4}\left[\frac{w_0''\phi_0''}{Re\upsilon e^{\xi}}\right]^{1/2}$$

where τ_w is the shear stress at the wall, q_w is the heat transfer at the wall, $Re=U_\infty L/\nu_0$, $w_0''=\left.\frac{\partial^2w}{\partial\eta^2}\right|_{\eta=0}$, and $\phi_0''=\left.\frac{\partial^2\phi}{\partial\eta^2}\right|_{\eta=0}$.

5. METHOD OF SOLUTION

The transformed initial boundary value problem, equations (25)–(31), is solved by a finite element–differential method. In essence, the method converts the partial differential equations into a system of ordinary differential equations by a weighted residuals method and invokes an ordinary differential equation solver for the numerical integration of the reduced initial-value problem. The boundary conditions at infinity, equation (30), are imposed at a sufficiently large finite distance, H, from the body surface.

For a selected H, the initial boundary value problem considered is governed by non-linear

parabolic partial differential equations of the form

$$w_\xi = W(\eta, w, w_\eta, w_{\eta\eta}, \phi) \tag{32}$$

$$\phi_\xi = \Phi(\eta, w, w_\eta, w_{\eta\eta}, \phi, \phi_\eta, \phi_{\eta\eta}) \tag{33}$$

$$k_\xi = K(\xi, \eta, k, k_\eta, k_{\eta\eta}, w, w_\eta, \varepsilon) \tag{34}$$

$$\varepsilon_\xi = E(\xi, \eta, \varepsilon, \varepsilon_\eta, \varepsilon_{\eta\eta}, w, w_\eta, w_{\eta\eta}, k) \tag{35}$$

where the subscripts ξ and η denote partial derivatives and W, Φ, K, E are non-linear differential operators given by the right hand sides of equations (25), (26), (27) and (28), respectively. The associated boundary and initial conditions are

$$w(\xi, 0) = 0, \phi(\xi, 0) = 0, k(\xi, 0) = 0, \varepsilon(\xi, 0) = 0 \tag{36}$$

$$w_\eta(\xi, 0) = 0, \phi_\eta(\xi, 0) = 0, k_\eta(\xi, 0) = 0, \varepsilon_\eta(\xi, 0) = 0 \tag{37}$$

$$w(\xi, H) = 1, \phi(\xi, H) = 1, k(\xi, H) = k_e(\xi), \varepsilon(\xi, H) = \varepsilon_e(\xi) \tag{38}$$

$$w_\eta(\xi, H) = 0, \phi_\eta(\xi, H) = 0, k_\eta(\xi, H) = 0, \varepsilon_\eta(\xi, H) = 0 \tag{39}$$

$$w(\xi_0, \eta) = w_i(\eta), \phi(\xi_0, \eta) = \phi_i(\eta) \tag{40}$$
$$k(\xi_0, \eta) = k_i(\eta), \varepsilon(\xi_0, \eta) = \varepsilon_i(\eta)$$

The additional boundary conditions given in equations (37) and (39) resulted from the physical boundary conditions and the transformations.

Interpolation functions

In the present study, the unknown functions $w(\xi, \eta)$, $\phi(\xi, \eta)$, $k(\xi, \eta)$, $\varepsilon(\xi, \eta)$ at a longitudinal station are represented by complete cubic splines. Let $f(\xi, \eta)$ denote any of the unknown functions $w(\xi, \eta)$, $\phi(\xi, \eta)$, $k(\xi, \eta)$, $\varepsilon(\xi, \eta)$ to be approximated by a complete cubic spline at a longitudinal station. Suppose that the interval $0 \leqslant \eta \leqslant H$ is properly discretized into n elements with $n + 1$ nodal points at $0 = \eta_1 < \eta_2 < \ldots < \eta_n < \eta_{n+1} = H$. Denote the value of $f(\xi, \eta)$ and its derivative with respect to η at nodal points η_i as

$$f(\xi, \eta_i) = f_i(\xi), \left.\frac{\partial f}{\partial \eta}\right|_{\eta = \eta_i} = f_i'(\xi)$$

For the ith element one defines the element size h_i as

$$h_i = \eta_{i+1} - \eta_i$$

and the local co-ordinate z as

$$z = \eta - \eta_i \quad 0 \leqslant z \leqslant h_i$$

Then, the cubic spline approximating $f(\xi, \eta)$ at a longitudinal station is given by

$$\bar{f}(\xi, \eta) = \sum_{i=1}^{n} \delta_i \bar{f}_i(\xi, z) \tag{41}$$

where

$$\delta_i = \begin{cases} 1, \text{ when } \eta_i < \eta < \eta_{i+1} \\ 0, \text{ otherwise} \end{cases}$$

and $\bar{f}_i(\xi, z)$, the cubic polynomials approximating $f(\xi, \eta)$ in the ith element, is given by

$$\bar{f}_i(\xi, z) = \sum_{j=1}^{n+1} a_{i,j}(z) f_j(\xi) + b_{i,1}(z) f'_1(\xi) + b_{i,n+1}(z) f'_{n+1}(\xi) \tag{42}$$

where $a_{i,j}(z)$, $b_{i,1}(z)$ and $b_{i,n+1}(z)$ are known polynomials of degree three in z. It should be noted that the cubic spline $\bar{f}$ agrees with f at the nodes and is twice continuously differentiable in the interval of interest, $0 < \eta < H$.

A method of weighted residuals

Owing to boundary conditions (37) and (39), equation (42) becomes

$$\bar{f}_i(\xi, z) = \sum_{j=1}^{n+1} a_{i,j}(z) f_j(\xi) \tag{43}$$

Furthermore, if the value of $f(\xi, \eta)$ is given at $\eta = 0$ and $\eta = H$ the unknowns to be determined in (43) are $f_2(\xi), \ldots, f_\eta(\xi)$. Substituting equation (43) into equation (41) one obtains

$$f(\xi, \eta) \simeq \bar{f}(\xi, \eta) = \sum_{j=2}^{n} N_j(\eta) f_j + F(\eta) f_{n+1}$$

where

$$N_j(\eta) = \sum_{i=1}^{n} \delta_i a_{i,j}(z) \text{ and } F(\eta) = N_{n+1}(\eta) = \sum_{i=1}^{n} \delta_i a_{i,n+1}(z).$$

For the application of the method of weighted residuals we chose weight functions equal to the interpolation functions (Galerkin's method). Accordingly, we obtain the following system of equations:

$$\sum_{j=2}^{n} \left[\sum_{i=1}^{n} \int_0^{h_i} a_{i,m}(z) a_{i,j}(z)\, \mathrm{d}z \right] \frac{\mathrm{d}w_j}{\mathrm{d}\xi} = \sum_{i=1}^{n} \int_0^{h_i} a_{i,m}(z) W_i\, \mathrm{d}z \tag{44}$$

$$\sum_{j=2}^{n} \left[\sum_{i=1}^{n} \int_0^{h_i} a_{i,m}(z) a_{i,j}(z)\, \mathrm{d}z \right] \frac{\mathrm{d}\phi_j}{\mathrm{d}\xi} = \sum_{i=1}^{n} \int_0^{h_i} a_{i,m}(z) \Phi_i\, \mathrm{d}z \tag{45}$$

$$\sum_{j=2}^{n} \left[\sum_{i=1}^{n} \int_0^{h_i} a_{i,m}(z) a_{i,j}(z)\, \mathrm{d}z \right] \frac{\mathrm{d}k_j}{\mathrm{d}\xi} = \sum_{i=1}^{n} \int_0^{h_i} a_{i,m}(z) K_i\, \mathrm{d}z - \frac{\mathrm{d}k_e}{\mathrm{d}\xi} \left[\sum_{i=1}^{n} \int_0^{h_i} a_{i,n+1}(z) a_{i,m}(z)\, \mathrm{d}z \right] \tag{46}$$

$$\sum_{j=2}^{n} \left[\sum_{i=1}^{n} \int_0^{h_i} a_{i,m}(z) a_{i,j}(z)\, \mathrm{d}z \right] \frac{\mathrm{d}\varepsilon_j}{\mathrm{d}\xi} = \sum_{i=1}^{n} \int_0^{h_i} a_{i,m}(z) E_i\, \mathrm{d}z - \frac{\mathrm{d}\varepsilon_e}{\mathrm{d}\xi} \left[\sum_{i=1}^{n} \int_0^{h_i} a_{i,n+1}(z) a_{i,m}(z)\, \mathrm{d}z \right] \tag{47}$$

In the above equations W_i is given by

$$W = W\left(z, \bar{w}_i, \frac{\partial \bar{w}_i}{\partial z}, \frac{\partial^2 \bar{w}_i}{\partial z^2}, \bar{\phi}_i \right)$$

Similar relations hold for Φ_i, K_i and E_i. The system of $4(n-1)$ equations, (44)–(47), can be written

in the matrix form

$$\begin{aligned}\left\{\frac{d\mathbf{w}}{d\xi}\right\} &= [\mathbf{Q}]^{-1}\{\mathbf{r}_1\}\\ \left\{\frac{d\boldsymbol{\phi}}{d\xi}\right\} &= [\mathbf{Q}]^{-1}\{\mathbf{r}_2\}\\ \left\{\frac{d\mathbf{k}}{d\xi}\right\} &= [\mathbf{Q}]^{-1}\{\mathbf{r}_3\}\\ \left\{\frac{d\boldsymbol{\varepsilon}}{d\xi}\right\} &= [\mathbf{Q}]^{-1}\{\mathbf{r}_4\}\end{aligned} \tag{48}$$

where $[\mathbf{Q}]$ is an $(n-1)$ by $(n-1)$ constant non-singular matrix which depends on the selected element discretization model, $\{\mathbf{w}\}^T = [w_2, w_3, \ldots, w_n]$, $\{\boldsymbol{\phi}\}^T = [\phi_2, \phi_3, \ldots, \phi_n]$, $\{\mathbf{k}\}^T = [k_2, k_3, \cdots, k_n]$, $\{\boldsymbol{\varepsilon}\}^T = [\varepsilon_2, \varepsilon_3, \cdots, \varepsilon_n]$ and the ith elements of the vectors $\{\mathbf{r}_1\}$, $\{\mathbf{r}_2\}$, $\{\mathbf{r}_3\}$ and $\{\mathbf{r}_4\}$ are given by the expressions on the right hand sides of equations (44), (45), (46) and (47), respectively. Consequently, the initial-value problem to be solved is

$$\begin{aligned}\left\{\frac{d\mathbf{Z}}{d\xi}\right\} &= [\mathbf{G}]\{\mathbf{r}\}\\ \{\mathbf{Z}(\xi_0)\} &= \{\mathbf{Z}_0\}\end{aligned} \tag{49}$$

where

$$\{\mathbf{Z}\}^T = [\mathbf{w}, \boldsymbol{\phi}, \mathbf{k}, \boldsymbol{\varepsilon}]$$
$$\{\mathbf{r}\}^T = [\mathbf{r}_1, \mathbf{r}_2, \mathbf{r}_3, \mathbf{r}_4]$$

and

$$[\mathbf{G}] = \begin{bmatrix} [\mathbf{Q}]^{-1} & 0 & 0 & 0 \\ 0 & [\mathbf{Q}]^{-1} & 0 & 0 \\ 0 & 0 & [\mathbf{Q}]^{-1} & 0 \\ 0 & 0 & 0 & [\mathbf{Q}]^{-1} \end{bmatrix}$$

Computational remarks

In the process of numerical integration the definite integrals involving W_i, Φ_i, K_i and E_i in equations (44)–(47) must be evaluated. The right hand sides of equations (32)–(35) are very complex, and explicit expressions for the above mentioned definite integrals cannot be obtained. These integrals are effectively evaluated by a Gauss-Legendre quadrature formula[24]

$$\int_{-1}^{1} F(\zeta)\, d\zeta \simeq \sum_{m=1}^{M} A_m^{(M)} F(\zeta_m^{(M)}) \tag{50}$$

in which $\zeta_m^{(M)}$ are the M zeros of the Mth degree Legendre polynomial and $A_m^{(M)}$ are weight factors associated with the Mth degree Legendre polynomial. In the present work the value $M = 6$ has been used in all computations.

The system (49) is moderately large and stiff. This is typical for systems of ordinary differential equations arising from the application of the method of lines to partial differential equations.[25] A discretization model for turbulent boundary layers at moderately high Reynolds numbers consists of 20 to 30 elements. This means that the solution of the initial boundary value problem, equations (25)–(31), with the proposed method give rise to systems of 96 to 116 ordinary

differential equations to be solved simultaneously. Owing to the presence of stiffness, conventional methods for numerical integration of the system (49) become inefficient and consequently methods suitable for stiff equations should be employed. In the present study a predictor–corrector method based on the backward difference formulae is used.[26]

The method described in this section has a definite advantage over conventional finite-difference methods in that the streamwise integration step size is automatically controlled by preassigned local error tolerance parameters.[27]

6. NUMERICAL RESULTS

The accuracy and efficiency of the numerical method as well as the predictive capability of the k–ε turbulence model have been investigated for a number of low speed, transonic and supersonic flows.

Low speed flows

As a preliminary effort, the high Reynolds number incompressible flow over a smooth flat plate at zero incidence has been considered. Since the computer program has been developed for compressible flows this case was treated as a very low subsonic flow over an adiabatic wall. To ensure the accuracy of the numerical solution, a number of numerical experiments have been conducted. It was found that $H = 8{\cdot}28$ is sufficiently large for imposing the outer boundary conditions. Moreover a 24-element discretization model with element size distribution $h_i =$ /3∗0·01, 2∗0·02, 0·03, 0·04, 0·06, 0·08, 0·1, 0·2, 0·3, 0·4, 8∗0·5, 3∗1/ has given very accurate results in the Reynolds number range $7 \times 10^5 \leqslant Re_x \leqslant 7 \times 10^7$. Figure 1 shows a comparison between the calculated local skin-friction coefficient (computations based on free-stream Mach number $M_e = 0{\cdot}044$) and von Kármán's empirical formula. The range $7 \times 10^5 \leqslant Re_x \leqslant 7 \times 10^7$ is covered in 37 steps. The size of the integration step in terms of the co-ordinate x in the physical plane is typically 5 to 15 times the local boundary-layer thickness. The CPU time needed is 280 s on an IBM 3033N

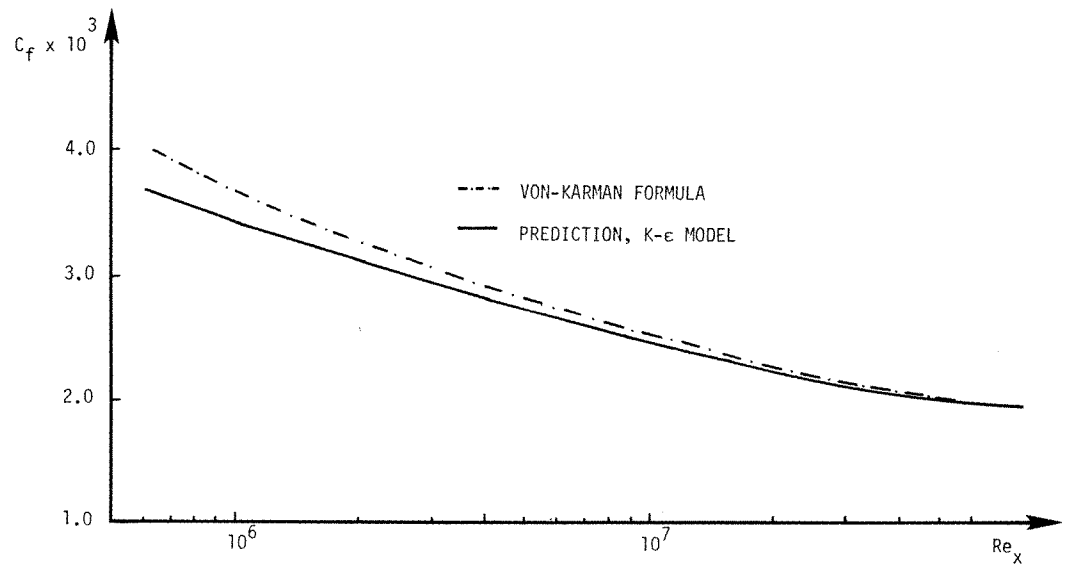

Figure 1. Comparison of calculated local skin-friction coefficient with von Kármán's formula

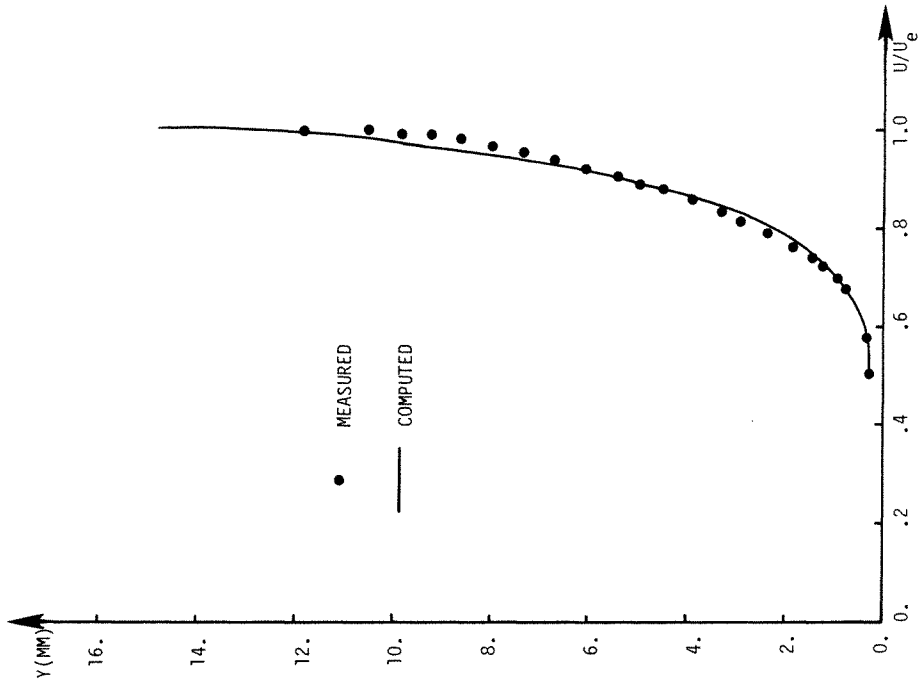

Figure 3. Mean velocity profile. Mabey–Meier–Sawyer flow
$M_e = 4{\cdot}5, Re_\theta = 15{,}000$

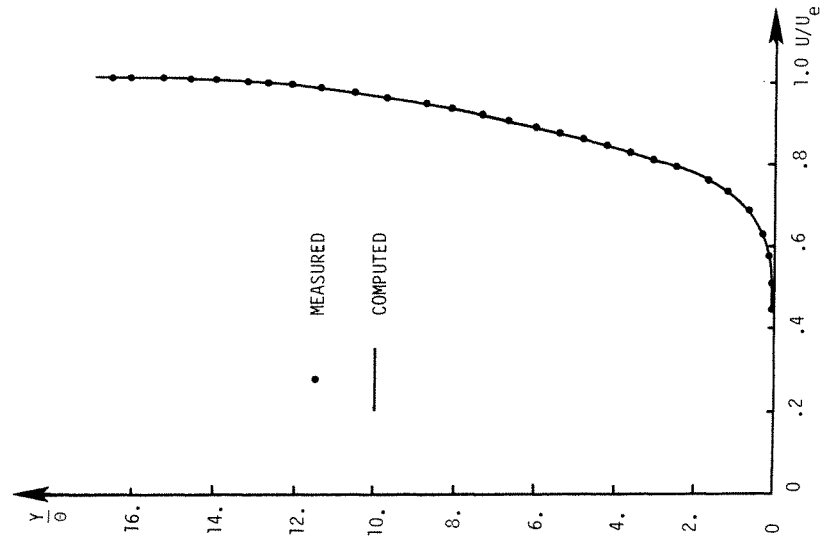

Figure 2. Mean velocity profile. Collins–Coles–Hicks flow
$M_e = 2{\cdot}18, Re_\theta = 40{,}500$

computer using double precision arithmetic. The method appears to be efficient considering the fact that integration of two-equation turbulence models by finite-difference methods requires very long CPU times.[28]

Supersonic flows

Figure 2 shows a comparison between the computed and experimental mean velocity profiles for the adiabatic boundary layer measured by Collins *et al.*[29] The agreement in this high Reynolds number experiment ($Re_\theta = 40{,}500$) is excellent. In the case of the data presented by Mabey *et al.*,[30] at $Re_\theta = 15{,}000$, very good agreement is achieved (Figure 3). However, the profile measured by Laderman and Demetriades,[31] at the low Reynolds number of $Re_\theta = 3400$ is very poorly 'predicted' (Figure 4). Table I lists the skin-friction coefficient, C_f, the boundary layer momentum thickness, θ, the shape factor $H_{12} = \delta^*/\theta$, and the kinematic shape factor $H_{12k} = \delta_k^*/\theta_k$ computed by the present method and those obtained from the measured data.

In the above, δ^* denotes the boundary-layer displacement thickness and subscript k denotes kinematic integral thickness. The various integral thickness are defined as follows:

$$\delta^* = \int_0^\infty \left(1 - \frac{\bar{\rho}\bar{u}}{\rho_e u_e}\right) dy, \quad \delta_k^* = \int_0^\infty \left(1 - \frac{\bar{u}}{u_e}\right) dy$$

$$\theta = \int_0^\infty \frac{\bar{\rho}\bar{u}}{\rho_e u_e}\left(1 - \frac{\bar{u}}{u_e}\right) dy, \quad \theta_k = \int_0^\infty \frac{\bar{u}}{u_e}\left(1 - \frac{\bar{u}}{u_e}\right) dy$$

The agreement with the experimental data is excellent for the high Reynolds number flows but deteriorates as the Reynolds number decreases.

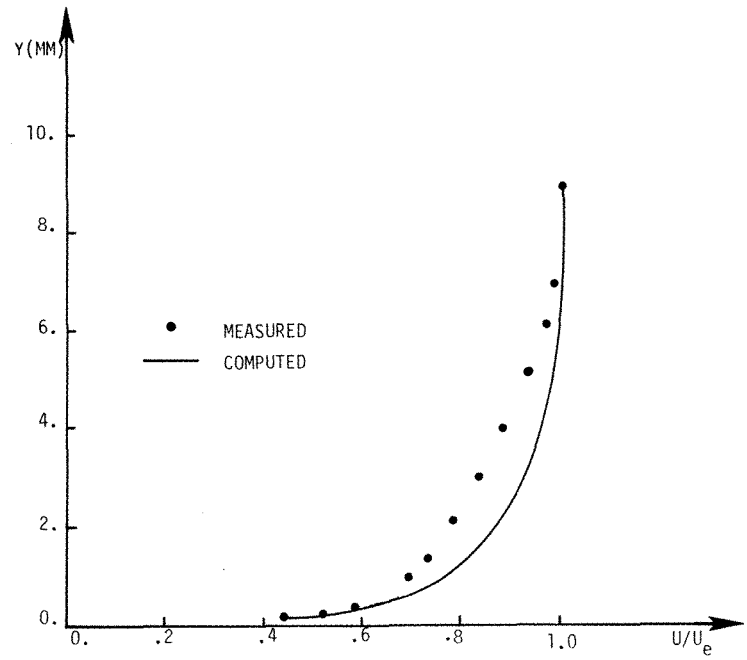

Figure 4. Mean velocity profile. Laderman–Demetriades flow

$M_e = 3{\cdot}0, Re_\theta = 3400$

Table I. Comparison between computed and measured boundary-layer parameters for several supersonic flows

	Collins–Coles–Hicks		Mabey–Meier–Sawyer		Laderman–Demetriades	
	$M_e = 2{\cdot}18$ Computed	$Re_\theta = 40{,}500$ From measurements	$M_e = 4{\cdot}5$ Computed	$Re_\theta = 15{,}000$ From measurements	$M_e = 3{\cdot}0$ Computed	$Re_\theta = 3400$ From measurements
$C_f 10^3$	1·41	1·45	0·87	0·98	1·97	1·96
θ (in mm)	2·21	2·24	0·535	0·527	0·312	0·535
H_{12}	3·23	3·10	9·99	8·61	5·44	5·44
H_{12k}	1·26	1·26	1·34	1·39	1·50	1·42

Transonic flows

The calculation of the boundary-layer flow experimentally documented by Baker and Squire[32] represents a more severe test of the turbulence model and the numerical method. In this experiment, the boundary-layer develops under the action of a sharp pressure rise associated with the presence of a shock wave. Furthermore, there is a strong favourable pressure gradient upstream of the interaction region. The static pressure distribution approximated by a least-squares cubic spline is shown in Figure 5. Figures 6 and 7 show the distribution of the boundary-layer momentum thickness, θ, and the boundary-layer shape factors, H_{12} and H_{12k}, as predicted by the present method. The agreement with the experimentally obtained values is good. Calculated mean velocity profiles upstream of the shock, in the interaction region, and downstream of the shock are compared with measured profiles in Figure 8. The results are generally better than those obtained by other turbulence models and reported in Reference 32.

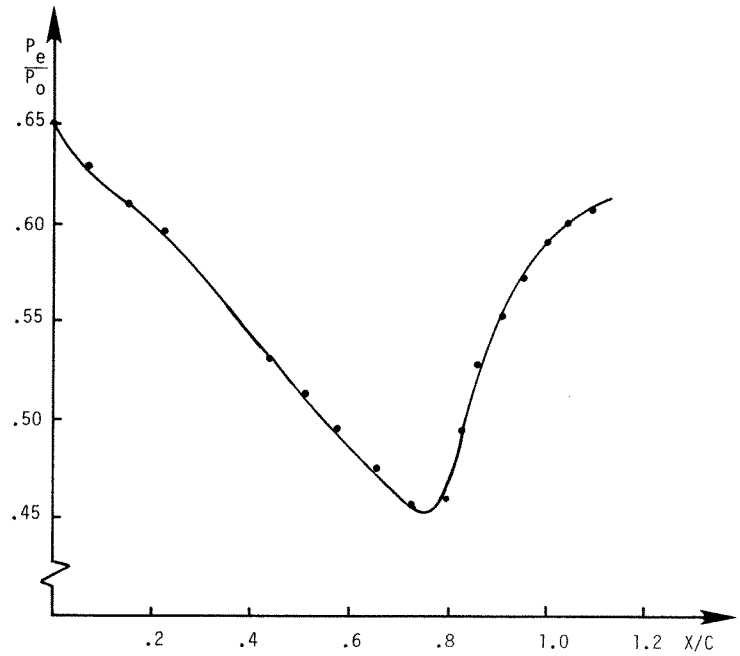

Figure 5. Static pressure distribution for Baker–Squire flow ($C = 0{\cdot}087$ m):———computed: ● measured

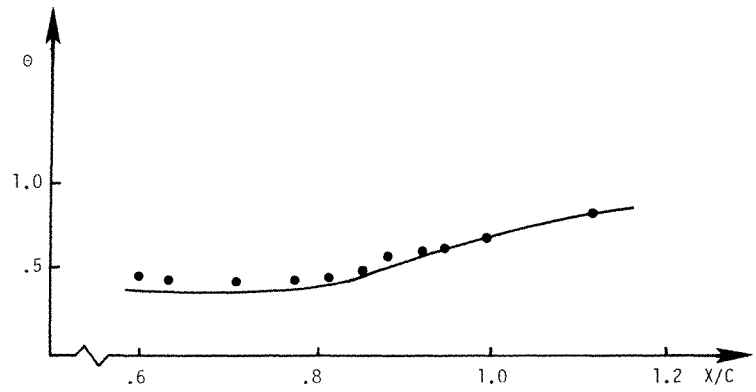

Figure 6. Boundary-layer momentum thickness. Baker–Squire flow ($C = 0{\cdot}087$ m): ——— computed; ● measured

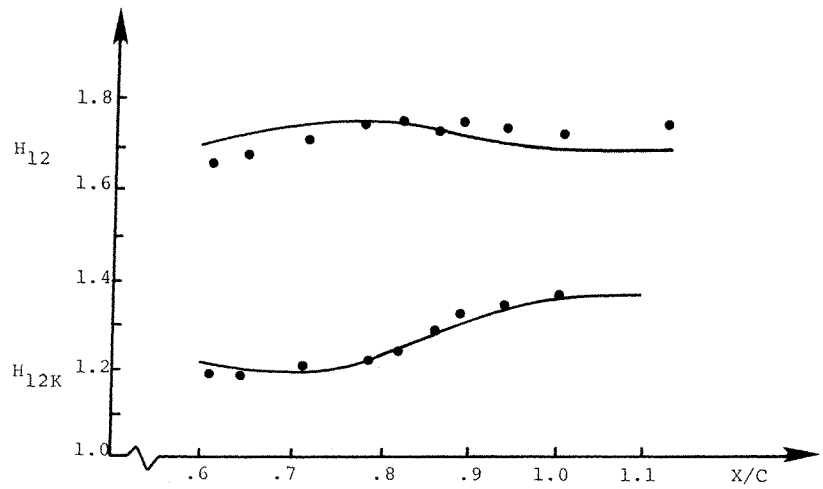

Figure 7. Boundary-layer shape factors. Baker–Squire flow ($C = 0{\cdot}087$ m): ——— computed; ● measured

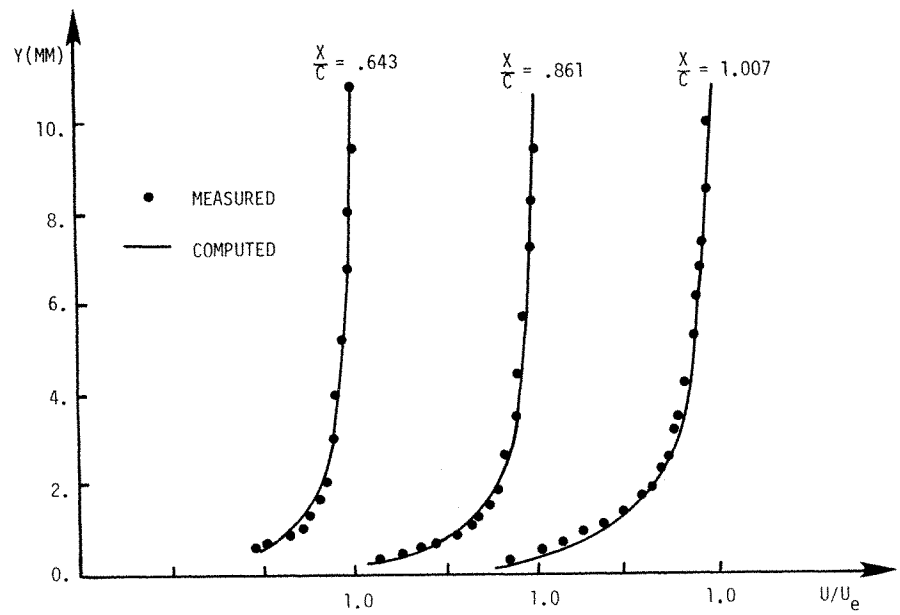

Figure 8. Mean velocity profiles. Baker–Squire flow ($C = 0{\cdot}087$ m)

7. CONCLUSIONS

A Galerkin procedure with the assumed solution profiles represented by complete cubic spline functions is applied to a number of low speed transonic and supersonic turbulent boundary-layer flows. The two-equations k–ε turbulence model is used in all computations. The results obtained show that the method can be efficient and provide highly accurate solutions over the entire boundary-layer region if sufficiently small elements are used close to the wall to resolve the steep gradients of the dependent variables in the viscous sublayer. Furthermore, the numerical results show that predictions based on the k–ε turbulence model are in good agreement with experimental data for attached non-hypersonic boundary layers. The computations exhibit excellent agreement with measurements at high Reynolds number flows but the accuracy of the predictions deteriorates as the Reynolds number decreases.

REFERENCES

1. T. J. Coakley, J. R. Viegas and C. C. Horstman, 'Evaluation of turbulence models for three primary types of shock separated boundary layers', *AIAA 10th Fluid & Plasma Dynamics Conference*, Albuquerque, N. Mexico, 1977.
2. S. E. Elghobashi and A. T. Wassel, 'The effect of turbulent heat transfer on the propagation of an optical beam across supersonic boundary/shear layers', *Int. J. Heat Mass Transfer*, **23,** 1229–1241, (1980).
3. D. R. Hartree and J. R. Womersley, 'A method for the numerical or mechanical solution of certain types of partial differential equations', *Proc. Roy. Soc. London*, **A161,** 353–366 (1937).
4. A. M. O. Smith and D. W. Clutter, 'Machine calculation of compressible laminar boundary layers', *AIAA Journal*, **3,** 639–647 (1965).
5. H. J. Herring and G. L. Mellor, 'A method of calculating compressible turbulent boundary layers', *NASA CR-1144*, 1968.
6. R. H. Pletcher, 'On a finite-difference solution for the constant-property turbulent boundary layer', *AIAA Journal*, **7,** 305–311 (1969).
7. R. H. Pletcher, 'Calculation method for compressible turbulent boundary-layer flows with heat transfer', *AIAA Journal*, **10,** 245–246 (1972).
8. J. E. Harris, 'Numerical solution of the equations for compressible laminar transitional and turbulent boundary layer and comparison with experimental data', *NASA TR-R-368*, 1971.
9. T. Cebeci, A. M. O. Smith and G. Mosinskis, 'Calculation of compressible adiabatic turbulent boundary layers', *AIAA Journal*, **8,** 1974–1982 (1970).
10. S. V. Patankar and D. B. Spalding, *Heat and Mass Transfer in Boundary Layers*, Intertext Books, London, 1970.
11. H. B. Keller and T. Cebeci, 'Accurate numerical method for boundary-layer flows—II two-dimensional turbulent flows', *AIAA Journal*, **10,** 1193–1199 (1972).
12. M. O. Soliman and A. J. Baker, 'Accuracy and convergence of a finite element algorithm for turbulent boundary layer flow', *Comp. Meth. Appl. Mech. Eng.*, **28,** 81–102 (1981).
13. C. A. J. Fletcher and R. W. Fleet, 'A Dorodnitsyn finite element formulation for turbulent boundary layers', *Proc. 8th Int. Conf. on Num. Meth. in Fluid Dynamics*, Aachen, 1982, published as *Lecture Notes in Physics*, **170,** Springer-Verlag, pp. 189–195.
14. C. C. Hsu, 'A finite element–differential method for a class of boundary-layer flows', *Proceedings of the 3rd International Conference on Finite Elements in Flow Problems*, Alberta, Canada, 1980.
15. C. C. Hsu and A. Liakopoulos, 'A finite element–differential method for a class of compressible laminar boundary-layer flows', in C. Taylor and B. A. Schrefler (eds), *Numerical Methods in Laminar and Turbulent Flow*, Pineridge Press, Swansea, U.K., 1981, pp. 497–504.
16. T. Cebeci and A. M. O. Smith, *Analysis of Turbulent Boundary Layers*, Academic Press, New York, 1974.
17. W. P. Jones and B. E. Launder, 'The calculation of low-Reynolds-number phenomena with a two-equation model of turbulence', *Int. J. Heat Mass Transfer*, **16,** 1119–1130 (1973).
18. W. P. Jones and B. E. Launder, 'The prediction of laminarization with a two-equation model of turbulence', *Int. J. Heat Mass Transfer*, **15,** 301–314 (1972).
19. D. C. Wilcox and M. W. Rubesin, 'Progress in turbulence modelling for complex flow fields including effects of compressibility, NASA TP 1517 (1980).
20. T. J. Coakley and J. R. Viegas, 'Turbulence modelling of shock separated boundary layer flows', *Symposium on Turbulent Shear Flows*, University Park, Pa., 1977.
21. P. Bradshaw, 'Compressible turbulent shear layers', *Ann. Rev. Fluid Mech.*, **9,** 33–54 (1977).
22. F. G. Blottner, 'Computational techniques for boundary layers', *AGARD-LS-73*, 1975.
23. A. Liakopoulos, 'A finite element-differential method for compressible turbulent boundary-layer flows', *Ph.D. dissertation*, University of Florida, 1982.

24. V. I. Krylov, *Approximate Calculation of Integrals*, Macmillan, New York, 1962.
25. A. C. Hindmarsh, 'ODE solvers for use with the method of lines', in R. Vichnevetsky and R. S. Stepleman (eds), *Advances in Computer Methods for Partial Differential Equations*—IV, IMASC, New Brunswick, N.J., 1981.
26. A. C. Hindmarsh, 'LSODE and LSODI, two new initial value ordinary differential equations solvers', *ACM-SIGNUM Newsletter*, **15,** 10–11 (1980).
27. A. Liakopoulos and C. C. Hsu, 'On a class of compressible laminar boundary-layer flows and the solution behaviour near separation', to appear in *J. Fluid Mechanics.*
28. D. C. Wilcox, 'Algorithm for rapid integration of turbulence model equations on parabolic regions', *AIAA Journal*, **19,** 248–250 (1981).
29. D. J. Collins, D. E. Coles and J. W. Hicks, 'Measurements in the turbulent boundary layer at constant pressure in subsonic and supersonic flow, Part I, Mean flow', *AEDC-TR-78-21*, 1978.
30. D. G. Mabey, H. U. Meier and W. G. Sawyer, 'Experimental and theoretical studies of the boundary layer on a flat plate at Mach numbers from 2.5 to 4.5', *RAE/TR 74127*, 1974.
31. A. J. Laderman, 'Effect of wall temperature on a supersonic turbulent boundary layer', *AIAA Journal*, **16,** 723–730 (1978).
32. C. J. Baker and L. C. Squire, 'Turbulent boundary-layer development on a two-dimensional aerofoil with supercritical flow at low Reynolds number', *Aeronautical Quarterly*, **XXXIII,** 174–198 (1982).